

# Modeling of Highly Flexible Structures

P. Frank Pai\*

University of Missouri–Columbia,  
Columbia, Missouri 65211

and

Mark J. Schulz†

North Carolina A&T State University,  
Greensboro, North Carolina 27411

## Introduction

RECENT rapid development in aerospace exploration has stimulated extensive use and studies of highly flexible structures (HFSs).<sup>1–4</sup> Figure 1 shows a representative load-deflection curve of HFS systems. It can have local buckling, snap-through, bifurcation, self-locking, snap-back, etc. Low-frequency vibration modes of HFSs are usually localized vibration modes, and hence local buckling is more likely to happen to HFSs. Local buckling results in significant load increase at some local areas, and hence plastic deformation may occur well before the entire structure collapses. For HFSs the design load can be chosen to be greater than the local buckling load, and hence the residual strength (the strength beyond the local buckling load) can be taken into account in the design. Snap-through happens when the load passes a limit point, and it causes serious dynamic effects. Hence, the load corresponding to the snap-through is often assumed to be the collapse load of an on-earth structure. However, if a structure can sustain the dynamic loads caused by the snap-through, the structure can be designed with a design load greater than the snap-through load. In this situation the dynamic effects caused by snap-through need to be carefully analyzed to ensure safety. Unfortunately dynamics of HFSs are essentially nonlinear because of high flexibility, and modal interactions caused by geometric nonlinearities would be the main cause of their complicated nonlinear dynamic responses, which is always a challenging problem. Moreover, multiple possible solution paths coexist around a bifurcation point of a load-deflection curve. To ensure structural safety, all of these possible solution paths need to be traced, which is a difficult numerical problem.

Some nonlinear behaviors of HFSs can be used to design large space structures. For example, the self-locking phenomenon can be used to design jointless deployable structures.<sup>3</sup> However, to push the design load beyond the local buckling load or even the snap-through point, it requires advances in modeling large deformations and complex stress states of HFSs, more efficient computational methods, and large static and dynamic tests to validate numerical simulations. Moreover, it is a new challenge to structural engineers to design large deployable/inflatable HFSs that can be packaged in a small volume for a space shuttle to carry and can be easily deployed or constructed in space.

Here we present some considerations and solutions to the modeling and design of HFSs based on the development and use of an in-house nonlinear finite element code.

## Modeling Issues

Approaches used in the literature in geometrically nonlinear modeling and finite element analysis can be grouped into four approaches: 1) an updated Lagrangian (UL) formulation using linear strains (e.g., engineering strains) defined with respect to the deformed configuration, 2) an UL-formulation using truncated nonlinear strain-displacement relations (e.g., von Kármán strains), 3) a total Lagrangian (TL) formulation using fully nonlinear strain-displacement relations (e.g., Green–Lagrange strains) derived by

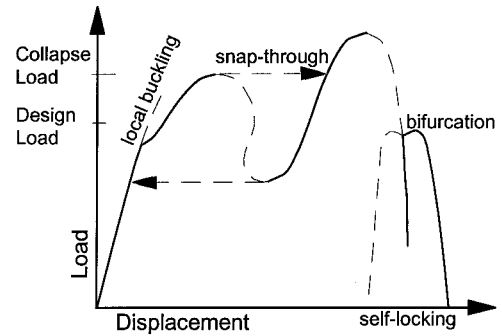


Fig. 1 Typical load-deflection curve of HFSs.

using large rotational degrees of freedom (DOFs), and 4) a TL-formulation using fully or truncated nonlinear strain-displacement relations (e.g., Green–Lagrange strains) defined with respect to a corotated elemental reference frame. Two approaches are commonly used in deriving fully nonlinear strain-displacement relations. The first one [used in approach 3)] uses three or two large Euler-type rotation angles as well as three displacement DOFs with respect to the undeformed reference frame.<sup>5</sup> Because finite rotation angles are not vector quantities, the derived strain-displacement relation is not invariant with respect to the rotation sequence. Hence, this approach is not appropriate for bifurcation study because some solutions can be prevented from being obtained if multiple solutions exist. Moreover, because the large rotational DOFs are usually treated as independent DOFs although they are functions of derivatives of translational DOFs, the orders of interpolation functions for rotational DOFs may not be consistent with those of translational DOFs. This inconsistency may cause the occur of spurious strains. Moreover, some finite elements derived from this approach use interpolation functions for in-plane displacements with orders lower than those for the out-of-plane displacements, which can cause spurious strains too. The second approach (used in approach 4) is to use three or two small Euler-type rotation angles or triads or quaternions as well as three displacement DOFs with respect to a corotated reference frame.<sup>6</sup>

Corotation is a method developed for making large rotations relative to an inertial frame look like small rotations at the element level.<sup>6</sup> The corotation is achieved by defining, for each element, a corotated reference coordinate frame using the deformed nodal coordinates. The rigid-body motion of this frame is then subtracted from the total motion of the nodes, leaving relative translations and rotations that can be made arbitrarily small by simply refining the mesh. Once nodal relative motions have been rendered sufficiently small, the relative small rotations can be treated as vector quantities, and they can be used in simplified strain-displacement relations. Nygard and Bergan<sup>7</sup> proved that the values of Green strains and second Piola–Kirchhoff stresses defined with respect to the undeformed frame are the same as those defined with respect to the corotated frame, and hence there is no need of transformation before updating these strains and stresses. However, the global displacements need transformation before updating. Moreover, because the corotated frame is defined by nodal coordinates, the sizes of elements need to be small in order to keep the relative rotations small.

The preceding discussion shows that a TL formulation with corotation is the most attractive approach, and fully nonlinear or truncated Green–Lagrange strains are commonly used in this approach.<sup>6,7</sup> Nonlinear strains used in a TL formulation need to be objective and geometric in order to use the material constants obtained from experiments in which rigid-body rotations are prevented and engineering stress and strain measures are used.<sup>8</sup> Unfortunately, Green–Lagrange strains are not geometric measures although they are objective.<sup>8</sup>

Pai and Palazotto<sup>9</sup> used Jaumann strains and new concepts of local relative displacements and orthogonal virtual rotations to derive a total-Lagrangian displacement-based finite element formulation of composite shells. In the formulation only global translational DOFs and their spatial derivatives are needed, and no relative rotational DOFs are used. Moreover, the formulation reveals that the order of interpolation functions for in-plane displacements needs to be the

Received 29 March 1999; revision received 9 March 2000; accepted for publication 12 March 2000. Copyright © 2000 by P. Frank Pai and Mark J. Schulz. Published by the American Institute of Aeronautics and Astronautics, Inc., with permission.

\*Associate Professor, Department of Mechanical and Aerospace Engineering. Member AIAA.

†Associate Professor, Department of Mechanical Engineering.

same as that for transverse displacements. Jaumann strains  $B_{ij}$  are defined as  $[B] \equiv [U] - [I]$ , where  $[I]$  is a unit matrix and  $[U]$  is the right stretch tensor that needs to be obtained from the deformation gradient tensor using the polar decomposition theory.<sup>8</sup> However, if  $\mathbf{u}(=0)$  represents the local relative displacement vector of an arbitrary point with respect to its deformed location, Jaumann strains  $B_{ij}$  can be proved to be<sup>8</sup>

$$B_{mn} = \frac{1}{2} \left( \frac{\partial \mathbf{u}}{\partial x_m} \cdot \mathbf{i}_n + \frac{\partial \mathbf{u}}{\partial x_n} \cdot \mathbf{i}_m \right) \tag{1}$$

where  $\partial x_j$  are unstrained lengths and  $\mathbf{i}_j$  are unit vectors along the convected coordinate axes only if shear strains are zero. If shear strains are nontrivial, a corotated point reference frame can be defined by using the symmetry of Jaumann strains.<sup>8</sup> Hence, Jaumann strains and stresses are along the corotated point reference frame at each point, and there is no need for a coordinate transformation before updating strains, stresses, and displacements. Using Eq. (1) and an exact coordinate transformation, Pai and Palazotto<sup>9</sup> showed that Jaumann strains can be presented in terms of global displacements without performing complex polar decomposition. Moreover, the energy formulation is usually used in the derivation of nonlinear structural theories without any correlation with the Newtonian formulation. Because Jaumann strains are geometric measures and can be presented in terms of vectors [see Eq. (1)], structural governing equations derived using the energy formulation are fully correlated with those derived using the Newtonian approach.<sup>9</sup> Furthermore, corotated Cauchy stresses and Eulerian strain rates are usually used in elastoplastic analysis, and their directions can be shown to be the same as those of Jaumann stress and Jaumann strain rates.<sup>8</sup> Hence the extension from geometrically nonlinear finite element analysis using Jaumann strains to elastoplastic finite element analysis is straightforward.

Based on the use of Jaumann stresses and strains, an exact coordinate transformation, and a new concept of orthogonal virtual rotations, geometrically exact structural theories have been derived and implemented in an in-house TL finite element code GESA

(geometrically exact structural analysis). Next we present some numerical results obtained from GESA to show the characteristics and challenging issues of HFSs.

Numerical Examples

Figure 2a shows the deformed configuration and projections of an isotropic circular band subjected to two opposite twisting moments  $\hat{M}_3$  at the two ends of a diameter with the left end at the origin and the right end being free to slide horizontally. The normalized

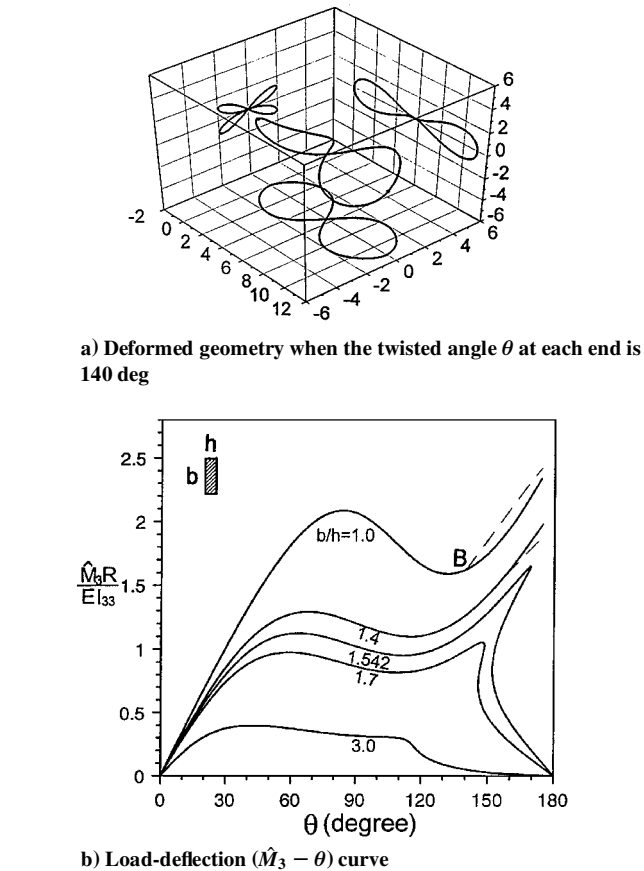
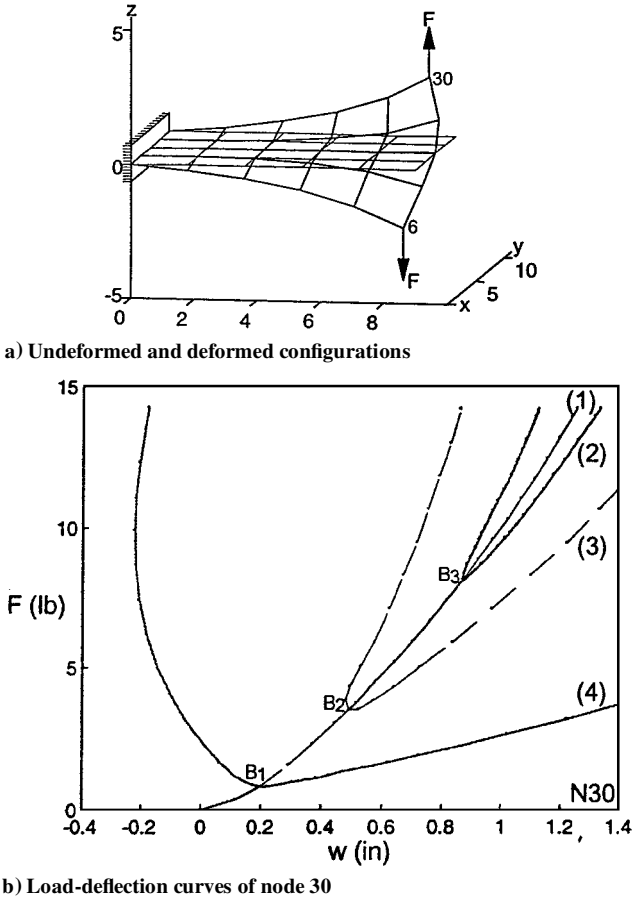


Fig. 2 Deformation of a circular isotropic ring subjected to two opposite twisting moments  $\hat{M}_3$  at the two ends of a diameter.

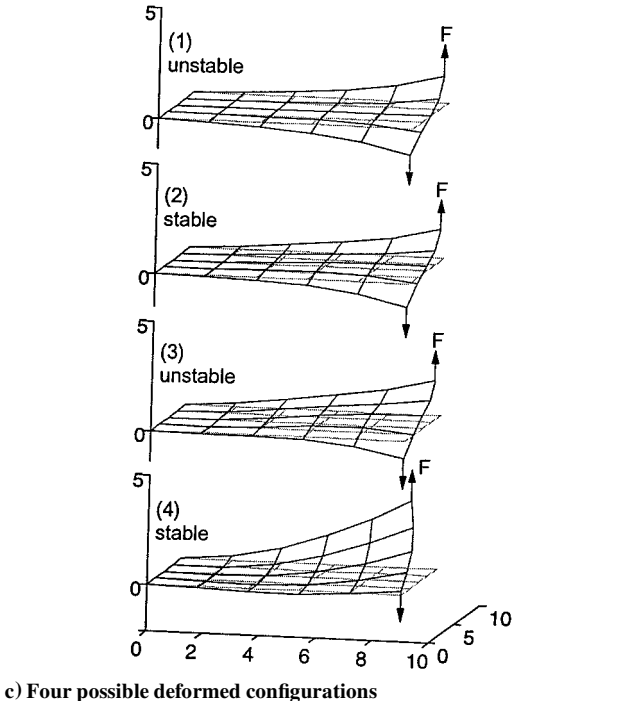


Fig. 3 Torsional deformation of a cantilevered rectangular plate subjected to two corner loads.

load-deflection curves in Fig. 2b show buckling, self-locking, contacting (point  $B$ ), and bifurcation phenomena. Here  $E$  is Young's modulus,  $I_{33}$  is the area moment of inertia,  $\theta$  is the twisting angle,  $R$  is the radius of the band, and  $b$  and  $h$  are the width and thickness of the cross section, respectively. The deformed geometry in Fig. 2a corresponds to point  $B$  ( $\theta = 140$  deg) in Fig. 2b, and it shows that the midpoint of the upper half ring is in contact with the midpoint of the lower half ring. If the ring is allowed to cut through itself (e.g., a half ring) when  $\dot{M}_3$  increases, the deformation follows the solid line in Fig. 2b. Otherwise, the load-deflection curve follows the broken line, and the upper and lower half rings start to tangle together. This contact problem is nonlinear. To prevent such impossible cut-through phenomena in analysis, the deformation path of every point of the structure needs to be checked against all other points because the neighboring points of an observed point vary when large displacements occur. Hence monitoring the deformation process using three-dimensional dynamic graphics is necessary for the analysis and design of HFSs. Moreover, the numerical results show that a ring can be twisted into three small rings with a diameter of one-third of the original diameter when  $2\theta = 360$  deg only if the cross-section aspect ratio  $b/h \geq 1.52$ . Figure 2b also shows the load-deflection curves with  $b/h = 1.542, 1.7$ , and  $3.0$ , where the deformed configurations at  $\theta = 180$  deg are self-locked because  $\dot{M}_3 = 0$ .

Figure 3a shows the undeformed and deformed configurations of a cantilevered rectangular isotropic plate subjected to two opposite transverse corner loads  $F$  when  $F = 316.31$  N. The dimensions are  $22.86 \times 17.78 \times 0.0660$  cm, Young's modulus  $E = 1.570 \times 10^{11}$  Pa, and Poisson's ratios  $\nu = 0.3$ . Figure 3b shows the several possible stable and unstable equilibrium paths of node N30, where  $w$  is the transverse displacement. Locating the bifurcation points  $B_1$ ,  $B_2$ , and  $B_3$  and tracing the bifurcated paths requires the development of special computational algorithms, which is an important but difficult task. The bifurcation points (especially  $B_1$ ) in Fig. 3b are the type of information important for the design of such HFSs. Figure 3c shows the four possible deformed configurations corresponding to (1), (2), (3), and (4) in Fig. 3b when  $F = 63.19$  N (i.e., one-fifth of the load used in Fig. 3a).

### Conclusion

In this Note we present some modeling, formulation, computation, and design issues of HFSs. Our numerical and experimental studies on HFSs show that transverse shear deformations, in-plane shearing, stretching, and thickness change are usually small. Other issues to be solved include measuring large deformations involving large rotations, influence of gravity, the use of initial stresses in design, and how to design loadings to have the required deformed shape (i.e., an inverse problem). Moreover, assembling TL finite elements of different types (i.e., cable, beam, plate, and/or shell elements) at a node but maintaining the geometrically exact formulation is still a challenging problem to be solved.

### References

- <sup>1</sup>Hedgepeth, J. M., "Interaction Between an Inflated Lenticular Reflector and Its Rim Support," AIAA Paper 95-1510, April 1995.
- <sup>2</sup>Greschik, G., "The Unfolding Deployment of a Shell Parabolic Reflector," AIAA Paper 95-1278, April 1995.
- <sup>3</sup>Szyszkowski, W., Youck, D., and Johnson, D. W., "The Dynamics of Deployment of a Satellite Boom with Self-Locking Joints," 15th Canadian Congress of Applied Mechanics, Univ. of Victoria, Victoria, BC, Canada, May–June 1995.
- <sup>4</sup>Greschik, G., and Park, K. C., "The Deployment of Curved Closed Tubes," AIAA Paper 95-1395, April 1995.
- <sup>5</sup>Surana, K. S., "Geometrically Nonlinear Formulation for the Curved Shell Elements," *International Journal for Numerical Methods in Engineering*, Vol. 19, No. 4, 1983, pp. 581–615.
- <sup>6</sup>Rankin, C. C., and Brogan, F. A., "An Element-Independent Corotational Procedure for the Treatment of Large Rotations," *Journal of Pressure Vessel Technology*, Vol. 108, No. 2, 1986, pp. 165–174.
- <sup>7</sup>Nygard, M. K., and Bergan, P. G., "Advances in Treating Large Rotations for Nonlinear Problems," *State-Of-The-Art Surveys on Computational Mechanics*, edited by A. K. Noor and J. T. Oden, American Society of Mechanical Engineers, New York, 1989, pp. 305–333.
- <sup>8</sup>Pai, P. F., Palazotto, A. N., and Greer, J. M., "Polar Decomposition

and Appropriate Strains and Stresses for Nonlinear Structural Analyses," *Computers and Structures*, Vol. 66, No. 6, 1998, pp. 823–840.

<sup>9</sup>Pai, P. F., and Palazotto, A. N., "Nonlinear Displacement-Based Finite-Element Analyses of Composite Shells—A New Total Lagrangian Formulation," *International Journal of Solids and Structures*, Vol. 32, No. 20, 1995, pp. 3047–3073.

R. B. Malla  
Associate Editor

## Avionics Module Recovery System for Expendable Launch Vehicles

Frederick W. Boltz\*  
NASA Ames Research Center,  
Moffett Field, California 94035

### Introduction

THE high cost of launch services is a serious problem for the U.S. commercial satellite industry and for NASA in the conduct of its scientific space program. In seeking a way to lower launch costs for small expendable launch vehicles (ELVs) using solid rocket motors (SRMs) in several stages, the idea of trying to recover the lower stages for reuse is not really practical, for a variety of reasons. Moreover, the value in recovering burned out SRM casings, nozzles, and control equipment from the lower stages is questionable. However, it does make sense to consider recovering all or part of the final stage, which includes the avionics module, in addition to the payload, SRM, and attitude-control equipment. The avionics module is the nerve center of the ELV and performs a variety of functions in vehicle guidance, navigation, and control (GN&C). In general, it contains an inertial measurement unit (IMU), a flight computer, a telemetry multiplexer, a telemetry transmitter, a flight-termination receiver, a radar transponder, reaction control system thrusters, other control units, and batteries in a relatively small volume. Advanced avionics architecture includes Global Positioning System microelectronics to enhance navigation and guidance of the final stage into a precise orbit. If the avionics module and related equipment could be recovered intact after each launch, with minimal cost and effort, it is believed that the savings in small ELV replacement costs could be substantial. Moreover, development of a practical avionics module recovery system could lead to a new kind of hybrid launch vehicle (HLV), which combines advantageous features of expendable and reusable systems. Such a partly reusable HLV might have a recoverable solid- or liquid-rocket final stage containing payload and avionics atop expendable solid- or liquid-rocket lower stages.

The purpose of this Note is to show how the avionics modules of two small ELVs could be recovered using miniature winged spacecraft incorporated into the final stage of each ELV. Because a detailed accounting of component costs for the small ELVs is proprietary information, it was not possible to quantify the cost benefit. That determination requires a definitive cost analysis, which includes an amortization of system development costs over a projected number of launches. In the final analysis, however, the decision of whether or not to proceed with concept development should not be based solely on economic considerations. There are other valid reasons for considering development of this kind of partly reusable launch system. Perhaps the most compelling reason is that both NASA and the U.S. Air Force would then have a cost-effective launch system with the capability of readily returning small scientific and military payloads from orbit.

Received 20 August 1999; revision received 24 January 2000; accepted for publication 24 January 2000. Copyright © 2000 by Frederick W. Boltz. Published by the American Institute of Aeronautics and Astronautics, Inc., with permission.

\*Aerospace Engineer, Aeronautics Division (retired). Member AIAA.